Instability and merging of a helical vortex pair in the wake of a rotor

Dominic Schröder, Thomas Leweke, Ralf Hörnschemeyer, Eike Stumpf

Instability and merging of a helical vortex pair in the wake of a rotor

D Schröder[1], T Leweke[2], R Hörnschemeyer[1] and E Stumpf[1]

[1]Institute of Aerospace Systems, RWTH Aachen University, 52062 Aachen, Germany
[2]IRPHE, CNRS, Aix-Marseille Université, Centrale Marseille, 13384 Marseille, France

E-mail: schroeder@ilr.rwth-aachen.de

Abstract. We present results from an experimental investigation of two closely spaced helical vortices. The two co-rotating vortices are generated in a water channel by a one-bladed rotor, whose tip geometry is modified by the addition of a perpendicular fin on the pressure side. The fin parameters are tuned so that the two vortices have approximately equal circulation. Dye visualisations and flow field measurements from Particle Image Velocimetry show that the vortices merge into a single tip vortex within less than one rotor rotation. This fast merging is caused by a rapid increase of the core radii of the initial vortices, which indicates the presence of an instability phenomenon. Analysis of the vortex velocity profiles identifies it as a centrifugal instability, linked to the presence of opposite-signed vorticity in the blade tip region. We further explore the origin of this vorticity by modifying the streamwise fin position. Measurements suggest that the interaction between the secondary fin vortex and the blade surface is partly responsible for the generation of the unstable velocity profile. The vortex resulting from the merging has a significantly larger core size than the one developing without a fin, indicating that this configuration could be beneficial in the context of Blade-Vortex Interaction noise for helicopters, or for the reduction of fatigue loads on wind turbine rotors caused by the interaction with concentrated tip vortices in the wake of upstream turbines.

1. Introduction

Many engineering application involve rotating blades, e.g. horizontal-axis wind turbines, helicopters and marine propellers. The flow generated by these rotor configurations is characterised by the existence of interlaced helical vortices emanating from the blade tips, which are a consequence of the lift force responsible for the thrust. These tip vortices remain concentrated in the early stages of the rotor wake evolution, and the associated high velocity gradients can lead to undesirable fluid-structure interactions. Regarding wind turbines, the unsteady loads induced on a blade by the vortex wake of a turbine located upstream can negatively affect performance and fatigue [1]. In the case of helicopters, rotor blades encountering the tip vortex of a preceding blade in certain flight regimes can generate unwanted noise (Blade-Vortex Interaction, or BVI, noise), as well as vibrations of the entire structure [2].

The unwanted high velocity gradients in the above interactions can be reduced by increasing the core size of the blade tip vortices. This strategy is followed in the current work, which involves a modified tip geometry used to generate two separate vortices, i.e. to split up and therefore spread out the associated vorticity distribution. This is achieved by adding a parametric fin, which is placed perpendicularly to the blade on the pressure side at a short distance from the

tip. Similar approaches have been pursued previously with different tip geometries (see, e.g., [3]), resulting in a measurable BVI noise reduction, but no detailed analysis of the involved flow phenomena was provided. One of these phenomena is vortex merging. Two closely-spaced like-signed vortices eventually merge into one single vortex in a viscous flow. The underlying physics have been investigated in various studies, e.g. in [4, 5] for the two-dimensional case, and in [6] for the merging of two co-rotating helical vortices. It was shown by Meunier et al. [7] that the merging process causes a significant change in the vortex characteristics, between the initial two vortices and the final merged vortex. The core radius $a_{\max}$, defined as the distance between the vortex centre and the point of maximum swirl velocity, is enlarged, whereas the peak vorticity in the vortex centre is reduced. In two-dimensional systems, the outcome of the merging is affected by the circulation ratio of the initial vortices and the distance between their centres. The final core radius is proportional to the vortex distance, and circulation ratios close to 1 lead to the largest values [8].

The onset of the merging process is governed by the ratio of the initial core size and the separation distance. Previous studies have deduced a critical ratio of the equivalent Gaussian core radius a, which is given by $a \approx a_{\max}/1.12$ [7], and the separation distance b_0, which is $a_c/b_0 = 0.24$ for the two-dimensional case [9]. For values higher than this limit, merging sets in. Cerretelli [5] has shown that the separation distance remains basically constant prior to the merging process. Therefore, the growth of the initial core radii represents the driving factor for reaching the critical merging ratio. For isolated vortices, this growth is mainly governed by the viscous diffusion of vorticity, which results in only a very slow increase at high Reynolds numbers. Faster growth can occur in the presence of (three-dimensional) instabilities that may arise from the interaction between the two initial vortices, and which generate small-scale turbulent motion in the core regions, thus enhancing the spreading of vorticity. For straight co-rotating vortices, the development of a short-wave elliptic instability in the vortices prior to merging was even found to reduce the critical onset ratio a_c/b_0 and produce a larger final core size [8, 10]. Helical vortex systems are also subject to long- and short-wave instabilities (with respect to the core size) [11], which can potentially contribute to an accelerated core growth in the present configuration.

The general concept of the blade modification described above has been investigated in detail in a previous experimental study [12]. It was shown, that certain fin configurations lead to a rapid merging process resulting in a strongly increased final core size. Depending on the circulation ratio of the two initial tip vortices, two scenarios were observed, which can be characterised as complete and partial merging. In the case of a complete merging, a rapid growth of the core radii, much faster than expected from viscous diffusion of vorticity, was found prior to the onset of the actual merging process, suggesting the existence of an instability phenomenon. With the time scales of the above-mentioned instabilities resulting from vortex interactions being incompatible with the observations, a closer analysis of the initial velocity profiles revealed that they were unstable with respect to centrifugal instability. This phenomenon, first described by Rayleigh [13], arises in vortices which are surrounded by a region of opposite-signed vorticity, resulting in a decrease of the absolute value of the circulation with increasing distance from the vortex centre. In these regions, the flow is unstable and characterized by three-dimensional perturbations. The theoretical work of Billant & Gallaire [14, 15] and Bayly [16] reviews this mechanism and its physical origin, and provides equations to determine the instability growth rate for generalised vortex velocity profiles, also including flow along the vortex axis. The values obtained with the experimentally measured profiles are compatible with the observed rapid growth of the initial core size, thus identifying centrifugal instability as a key element leading to a very fast merging in our configuration.

In the present contribution, we further explore the origin of the centrifugal instability. We first recall the evolution of the helical vortex pair generated by the finned rotor blade, showing the rapid and strong vortex core growth, compared to the unmodified rotor, and the evidence for

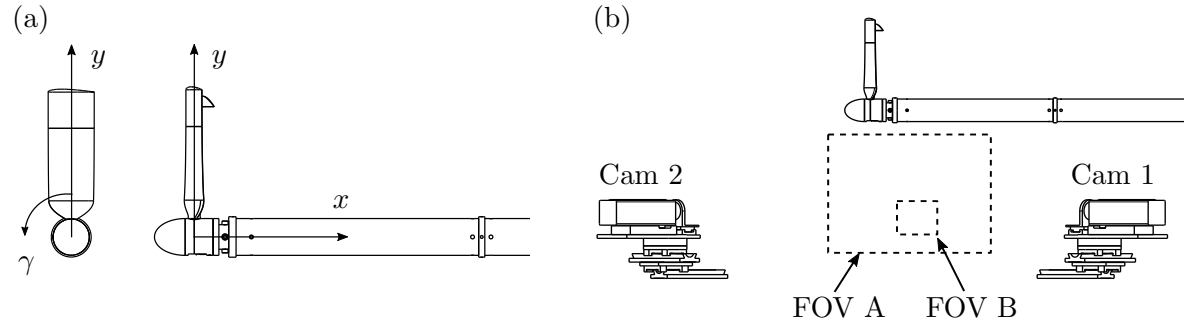

Figure 1. (a) Rotor set-up and coordinate system. The channel flow (free stream) is in the x-direction. (b) Fields of view (FOV) for the PIV measurements.

a centrifugal instability. We then present the results obtained from a series of experiments where the fin position is varied in the chordwise direction. These were carried out to test the hypothesis that the interaction between the fin vortex and the blade surface generates the opposite-signed vorticity leading to a centrifugally unstable flow.

2. Experimental details

Experiments were carried out in the large recirculating water channel of the Institue of Aerospace Systems. Its test section has dimensions of 1.5 m (width) × 1 m (height) × 6.5 m (length) and glass walls suitable for optical measurement techniques. The rotor used in this study consists of a single constant-chord blade with a NACA 0012 profile, whose twist distribution was determined for operation in conditions close to hover. In practice, a free-stream velocity of 11.5 cm/s was set in the water channel, in order to avoid a large-scale recirculation in the test section. To ensure a sufficiently large core size of the vortex forming at the rounded blade tip, for resolved Particle Image Velocimetry measurements, a relatively large chord length of $c = 80\,\mathrm{mm}$ was chosen. The rotor radius is $R = 240\,\mathrm{mm}$. The rotor is mounted on a shaft of diameter 60 mm, which has a length of 1.8 rotor diameters and is driven through a gear box by a motor outside the test section. Figure 1(a) shows a schematic of the set-up. The rotation frequency is $f = 1\,\mathrm{Hz}$, resulting in a Reynolds number based on the blade chord and tip velocity of $Re = 2\pi Rfc/\nu = 120\,000$ (ν: kinematic viscosity).

The blade tip was modified by adding a perpendicular fin on the pressure side, in order to generate a second tip vortex. The fin is rectangular and untwisted, and like the blade it has a NACA 0012 profile and a rounded tip. The various parameters defining the fin dimensions and position are shown in Fig. 2(a). The outer 60 mm of the blade (designated by the length l in the figure) were interchangeable, to allow for a simple adaptation of various geometric configurations with different fin parameters, each of which was manufactured by rapid prototyping. In a preliminary study, a large number of parameter combinations were tested (see, e.g., [12]). The configuration used in the present analysis has a fin-to-blade tip distance $d = 0.2c$, fin chord $c_f = 0.8c$, fin height $h = 0.3c$ and fin angle $\alpha_f = 14°$. For these values, the circulations of the blade and fin tip vortices were found to be approximately equal. In addition to this reference case, three other geometries were considered, where the fin position along the chordwise direction was varied. They are shown schematically in Fig. 2(b). They can be identified by the distance t between the trailing edges of the fin and the blade, counted positive in the downstream direction. Including the reference case, four positions were thus tested in the range $-0.2c \leq t \leq 0.2c$.

Stereoscopic Particle Image Velocimetry (SPIV) measurements were carried out to obtain the three components of the flow velocity in the symmetry plane of the rotor, which were used to determine the properties of the tip vortex system. Two CCD cameras (PCO.2000) with a spatial

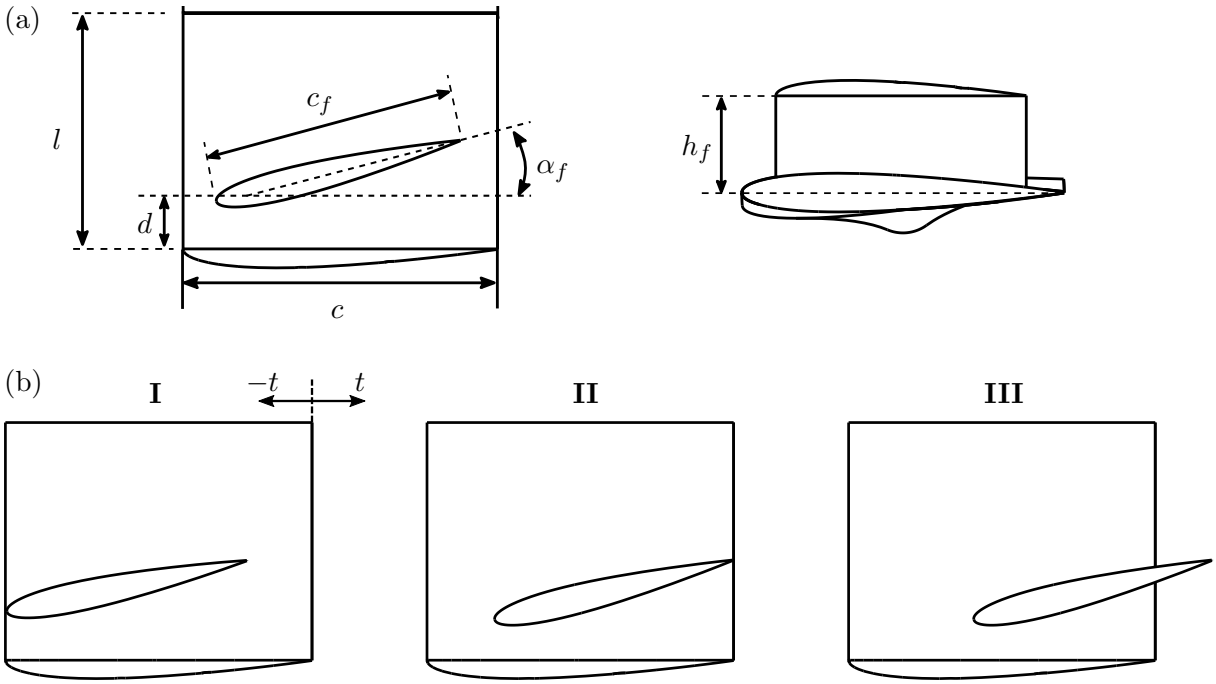

Figure 2. (a) Geometry of the primary interchangeable blade tip. (b) Configurations with different chordwise fin positions, the other parameters being unchanged.

resolution of 2048 × 2048 pixels were used for these measurements, for which flow illumination was achieved with a double-pulsed laser (Quantel Twins Ultra), providing a pulse energy of 120 mJ at a wavelength of 530 nm. The flow was seeded with cubic polyamide particles of mean diameter 50 µm and a density of 1.016 g/cm^3. Synchronised triggering of the cameras and laser at the desired rotor phase γ was achieved by an optical encoder combined with a micro-controller. Two fields of view (FOV) were investigated, shown schematically in Fig. 1(b). In a first step, the evolution of the vortex system was observed in the entire near-field wake with FOV A, spanning a 300 mm × 220 mm area. A smaller, square field of view (FOV B) with a side length of 80 mm, providing a higher spatial resolution in the relevant flow regions (determined from FOV A), could then be applied, in order to determine the vortex parameters more accurately. The temporal and spatial evolution of the vortices was recorded in 18° steps of the rotor angle γ, up to a final angle of $\gamma = 540°$. In order to compensate for the streamwise motion of the vortices and ensure that they are always well within the field of view, the position of the rotor was adjusted in the $x-$ and $y-$directions by means of linear axes. For each phase, 300 frames were captured using the double-frame/single-pulse technique. The calibration process, image acquisition, synchronization of cameras and laser, and processing of the images, were performed using the DaVis 8.4 software developed by LaVision.

3. Results

3.1. Effect of the fin on tip vortex evolution

We here briefly recall the key findings from a previous study presented in [12]. The additional fin and the resulting secondary vortex have a significant effect on the rotor wake evolution. Provided that the two tip vortices have similar circulations, a rapid merging into a final vortex of considerably larger core size than for the case without fin occurs. A qualitative impression of this effect can be seen in the dye visualisations in Fig. 3. These were obtained by injecting a solution of fluorescein through channels inside the blade and tip, and by illuminating the flow in

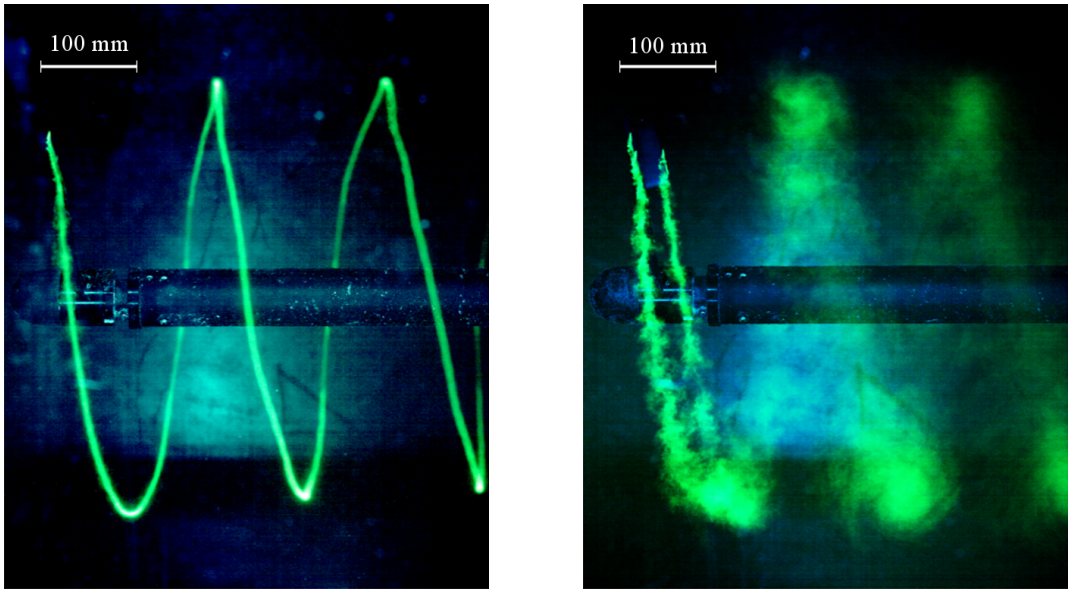

(a) Unmodified blade (b) Modified blade

Figure 3. Dye visualisations of the rotor wake. (a) Blade without fin; (b) blade with a fin having geometric parameters $d/c = 0.2$, $h/c = 0.3$, $c_f/c = 0.8$ and $\alpha_f = 14°$.

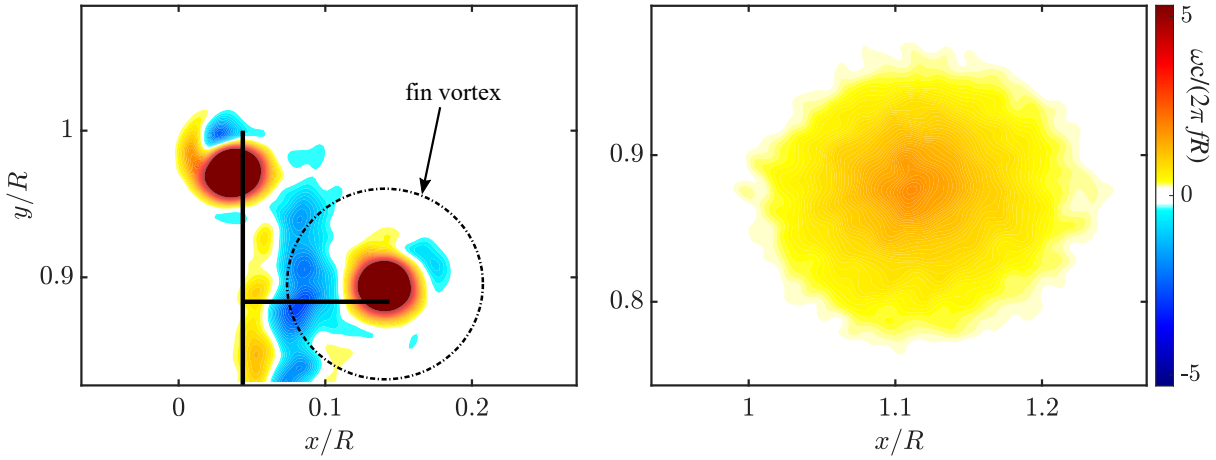

(a) $\gamma = 18°$ (b) $\gamma = 540°$

Figure 4. Phase-averaged vorticity in the centre plane of the rotor. (a) Initial vortex system; the black lines represent the trailing edges of the fin and the rotor blade, and the fin vortex is marked by a dashed circle. (b) Final merged vortex. The scale is the same in both images.

volume with ultraviolet light. In comparison to the stable and concentrated tip vortex generated by the unmodified blade, the wake of the modified rotor shows remarkable differences. Two vortices emanate from the blade and fin tips; they appear to be unstable, and they merge into a single vortex within about half a blade rotation. The dye pattern gives the impression that the core radius of the final merged vortex is considerably larger than the one of the single tip vortex at the same phase.

These qualitative observations are supported by the quantitative results from the PIV measurements. Figure 4 shows the phase-averaged fields of the azimuthal vorticity in the centre

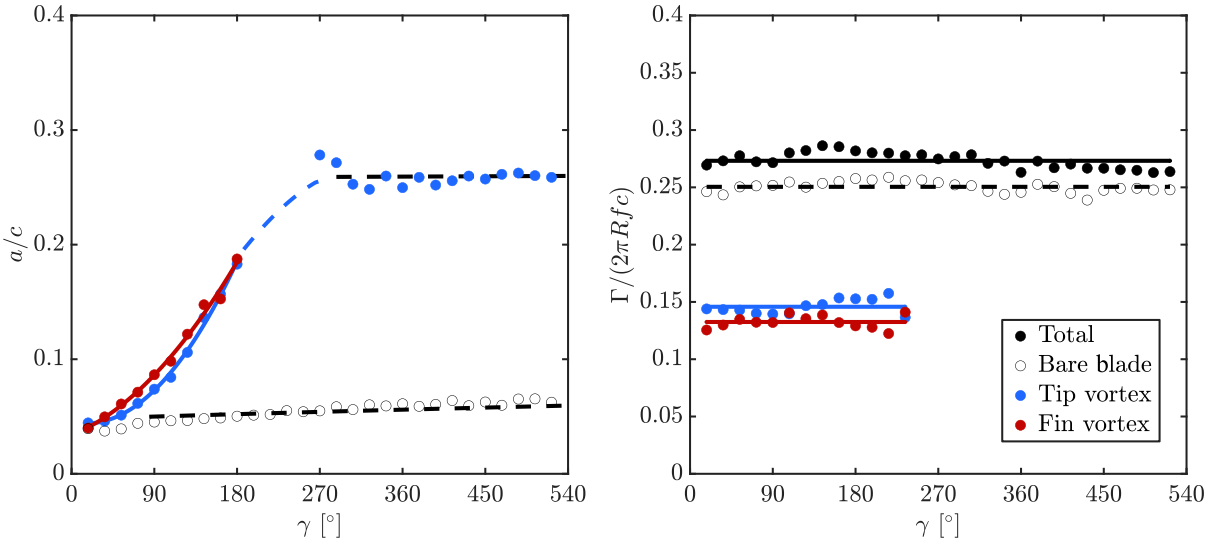

(a) Core radii (b) Circulations

Figure 5. Evolution of (a) the core radii and (b) the circulations (Γ) for the reference configuration. The dashed lines represent laminar core growth due to to viscous diffusion of vorticity.

plane of the rotor for the reference case with fin. Closely behind the blade, at $\gamma = 18°$, the two vortices are concentrated and well separated. After one and a half rotor rotations ($\gamma = 540°$), the newly formed single vortex has a vorticity distribution whose characteristic size is many times the initial core size. The peak vorticity is also only a fraction of the initial value.

In Fig. 5(a), the evolution of the core radii is presented. Starting immediately behind the blade, the radii of both vortices rapidly increase, at a rate which is much higher than expected from viscous diffusion of vorticity alone, which governs the evolution for the unmodified case. The critical ratio of core radius and separation distance is reached at $\gamma \approx 120°$, and the transformation of the vortex cores associated with their merging sets in. In the interval $180° < \gamma < 270°$, the cores are too deformed to determine their radii reliably. Once the merging is completed and a new, roughly axisymmetric vortex has formed, the core radius is about five times larger than for the case without fin, at the same downstream location. The further evolution appears to be governed by vorticity diffusion again. The circulation measurements in Fig. 5(b) show that the two initial vortices indeed have almost the same strength. The total circulation is constant, as expected. Its value is approximately 15% larger than for the blade without fin.

The strong increase in core size in the early helical vortex pair are linked to an instability of the vortices. The corresponding perturbations can be seen in the visualization of Fig. 3(b). The vorticity field in Fig. 4(a) shows that the concentrated fin vortex core is surrounded by regions of opposite-signed vorticity, which is an indicator for a centrifugally unstable situation. In order to compare with theoretical predictions concerning this instability, one can calculate axisymmetric velocity and circulation profiles for the fin vortex, by interpolating the PIV measurements onto a polar coordinate system centred on this vortex, and by averaging or integrating the swirl velocity on concentric circles of radius ρ. The radial circulation profile of the fin vortex at rotor phase $\gamma = 18°$, obtained in this way, is shown in Fig. 6(a). It exhibits a region ($0.1 < \rho/c < 0.25$) where the circulation decreases with increasing distance from the vortex centre, which is a sufficient condition for centrifugal instability. For larger distances, the circulation increases again.

The growth rate of centrifugal instability can be estimated from the (axisymmetric) profiles

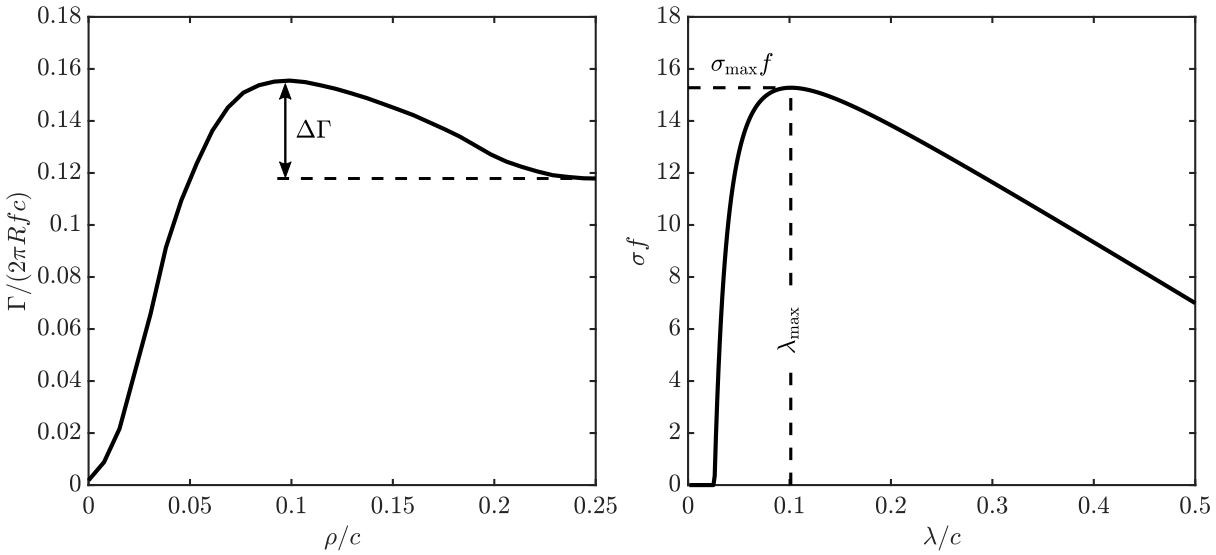

(a) Radial circulation profile (b) Centrifugal instability growth rate

Figure 6. (a) Radial circulation distribution of the fin vortex at $\gamma = 18°$. (b) Corresponding viscous growth rate of centrifugal instability, as function of the perturbation wavelength in the direction of the vortex axis.

of swirl velocity and axial velocity (along the vortex core), neglecting the large-scale curvature of the vortices. The procedure is based on the theoretical work of Billant & Gallaire [15] and Bayly [16]; details can be found in [12]. The result is shown in Fig. 6(b), where the growth rate, non-dimensionalised with the rotor period, is plotted as function of the perturbation wavelength in the direction of the vortex axis. The predicted most amplified wavelength is $\lambda_{\max} = 0.1c = 8$ mm, which is compatible with the scale of the perturbations visible in Fig. 3(b). The high value of the corresponding growth rate is also consistent with the observed rapid growth.

3.2. Origin of the centrifugal instability

The results of the previous section provide evidence that the helical vortex pair generated by the modified blade tip geometry undergoes a strong centrifugal instability immediately after its formation, due to the presence of counter-rotating vorticity in its vicinity. Concerning the origin of this opposite-signed vorticity, several hypotheses can be considered.

For a rotating blade of constant chord, the bound circulation responsible for the lift typically increases approximately linearly from the rotor centre (hub) along the span, reaching a maximum a short distance from the tip before falling sharply to zero at the tip itself. Such a circulation profile produces a concentrated vortex of one sign at the tip, and a constant-strength vortex sheet of the opposite sign behind the rest of the blade, since the trailing circulation is proportional to the radial gradient of bound circulation. This sheet provides one source of opposite-signed vorticity. The single vortex generated at the blade tip without fin is not unstable (see Fig. 3a); its core is not in close proximity to the vortex sheet. The fin vortex, however, is generated at some distance from the tip and may interact stronger with the vortex sheet of the other sign.

A second source of vorticity having a sign opposite to that of the tip vortices may arise from the interaction between the fin vortex and the blade surface. The fin vortex is generated along the fin tip, i.e. its initial part is parallel to the pressure surface of the blade. Due to the no-slip condition at this solid boundary, a velocity gradient appears near the surface from the difference between the flow induced by the vortex and the vanishing velocity at the wall, corresponding to

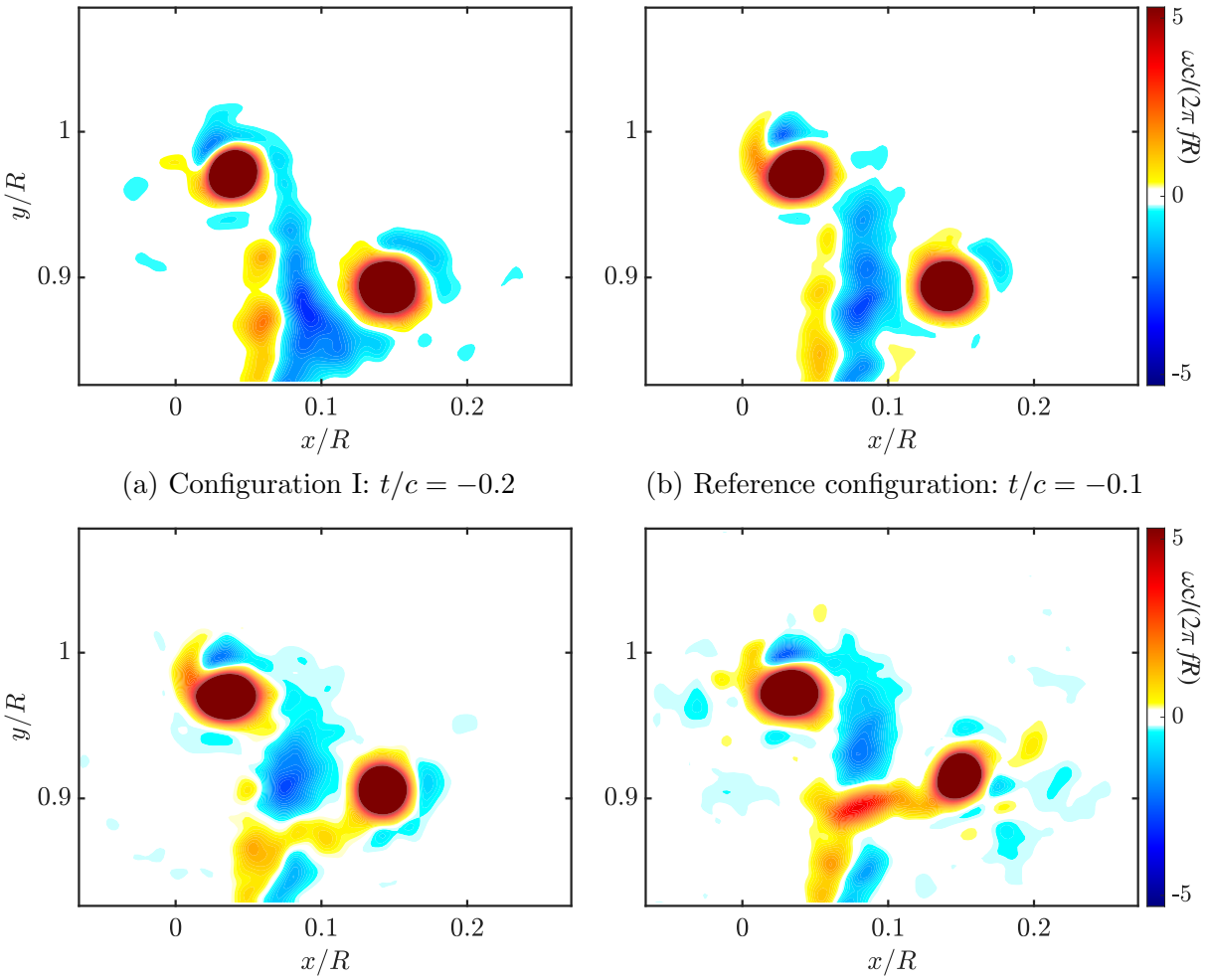

(a) Configuration I: $t/c = -0.2$

(b) Reference configuration: $t/c = -0.1$

(c) Configuration II: $t/c = 0$

(d) Configuration III: $t/c = 0.2$

Figure 7. Comparison of the initial vorticity fields (at $\gamma = 18°$) for various chordwise fin positions (see Fig 2).

a vorticity of opposite sign. The resulting circulation is convected away from the blade, along with the vortex. It can then be wrapped around the fin vortex, leading to instability. This mechanism is expected to be affected by the position of the fin along the blade chord. A position closer to the leading edge of the blade should have a greater interaction potential, since the fin vortex encounters a larger portion of the blade while propagating downstream. On the other hand, displacing the fin closer to the trailing edge, or even beyond, is expected to reduce this interaction.

In order to explore the second hypothesis, a series of experiments were carried out with the fin placed at various chordwise positions (see Fig. 2b). All other fin and flow parameters remained unchanged. The total circulation was found to vary only slightly (within a few percent) between these configurations. Figure 7 shows the initial phase-averaged vorticity fields for the four cases tested. When the fin is flush with the leading edge of the blade (configuration I in Fig. 2b), an extended zone of negative vorticity is seen, which appears to originate at the blade surface (Fig. 7a). As the fin position moves downstream, this region decreases in size and intensity, which is consistent with the proposed scenario.

A more quantitative assessment can be made by plotting the circulation decrease $\Delta\Gamma$, defined

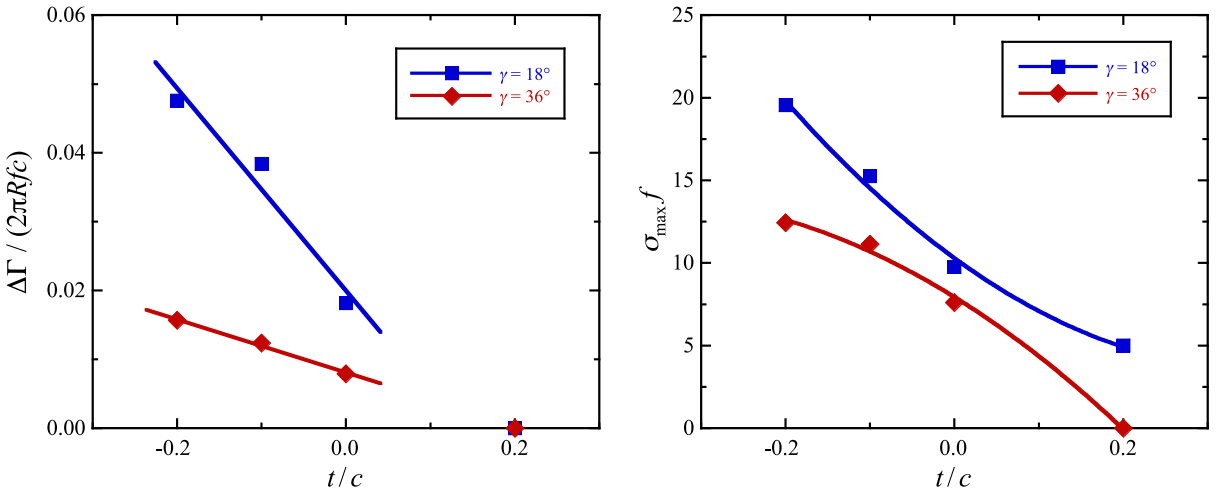

(a) Circulation decrease (b) Growth rate

Figure 8. Influence of the fin position t/c on (a) the radial circulation decrease $\Delta\Gamma$ and (b) the predicted maximum centrifugal instability growth rate, determined from the velocity fields measured at rotor phases $\gamma = 18°$ and $36°$.

in Fig. 6(a), as function of the fin position t. The result in Fig. 8(a) clearly shows the decrease of the opposite-signed circulation, as the fin moves towards the trailing edge of the blade. For configuration III, where the fin extends beyond the blade, no decrease is found in the radial circulation profile of the fin vortex. Figure 8(b) shows the corresponding maximum growth rate of the centrifugal instability, predicted as above from the measured fin vortex velocity profiles. It qualitatively behaves as $\Delta\Gamma$. Interestingly, it is still positive for $t/c = 0.2$ and $\gamma = 18°$, despite the absence of a radial circulation decrease. This can be explained from theory [15] by the presence of an axial velocity along the fin vortex. Further behind the blade (at $\gamma = 36°$), the flow is globally less unstable.

These results show that the chordwise fin position has a pronounced impact on the initial vorticity fields and the corresponding growth rates of the centrifugal instability, and that therefore the interaction between fin vortex and blade surface provides a plausible explanation for this behaviour. Measurements of the core radius evolution for the different fin positions considered here, have nevertheless shown only slight variations in the size of the final merged vortex. The latter is likely to be influenced mainly by the initial separation distance of the vortex pair, due to the conservation of angular momentum.

As mentioned at the beginning of this section, opposite-signed circulation leading to centrifugal instability may also come from the vorticity sheet shed behind the inner part of the blade. One might therefore expect an additional influence of the distance between fin and blade tip (d in Fig. 2a) on the instability characteristics. Testing this idea is more complicated, however, since the circulations of both tip and fin vortices, as well as their ratio, were found to vary quite significantly with d/c [12], making it hard to isolate the effect of only the fin vortex position with respect to the vorticity sheet.

4. Conclusion

We have presented results from an experimental study of the flow around a one-bladed rotor with a special tip geometry involving a parametric fin mounted on the pressure side of the rotor blade, which generates two separate tip vortices in its wake. From the start, the two helical tip vortices exhibit an intense three-dimensional instability, leading to a rapid increase of their

core size, and their subsequent merging into a single helical vortex within less than one rotor rotation. The final vortex has a significantly larger core size than the tip vortex for the same blade without fin. This also implies a lower vorticity peak and smaller velocity gradients, which make potential fluid-structure interactions with another blade or rotor less hazardous. The proposed tip geometry may therefore have potential as a method to reduce helicopter noise or fatigue loads on wind turbines aligned with the wind direction. The induced modifications of the tip vortices may also have an influence on other phenomena involved in the evolution of the rotor wake, such as the long-wave pairing instability [11]. Even if variations of the core size have only a small effect on the growth rate of this instability, the increased total circulation and higher perturbation level resulting from the turbulent merging may enhance its development and lead to a shorter characteristic length of the rotor near wake.

The analysis of the vorticity field and the vortex velocity profiles provides evidence that a centrifugal instability is responsible for the rapid initial core growth. Further experiments showed that the interaction between the fin vortex and the blade surface produces the opposite-signed vorticity leading to a centrifugally unstable flow. Another source of such vorticity may be the vortex sheet trailing behind the inner span of the blade.

The tip vortex cores also feature a velocity component directed along their axis, towards the blade (velocity defect). As the core size increases sharply due to the perturbations from the centrifugal instability, the ratio between swirl velocity and maximum axial velocity, i.e. the swirl number, decreases and may reach values below the limit for another type of vortex instability, the swirling jet instability (see, e.g., Ash & Khorrami [17]). This phenomenon may therefore also contribute to the acceleration of the merging process observed in the present configuration. Further experiments are planned, including three-dimensional tomographic PIV measurements, in order to clarify the role of the various physical mechanisms acting during the evolution of the helical vortex pair.

Acknowledgments

This work is part of the German-French project TWIN-HELIX, supported by the *Deutsche Forschungsgemeinschaft* (grant no. 391677260) and the French *Agence Nationale de la Recherche* (grant no. ANR-17-CE06-0018).

References

[1] Zhao R, Shen W, Knudsen T and Bak T 2012 *Wind Energy* **15** 927
[2] Yu Y H 2000 *Progr. Aerosp. Sci.* **36** 97
[3] Brocklehurst A and Barakos G N 2013 *Prog. Aerosp. Sci.* **56** 35
[4] Melander M V, Zabusky N J and McWilliams J C 1988 *J. Fluid Mech.* **195** 303
[5] Cerretelli C and Williamson C H K 2003 *J. Fluid Mech.* **475** 41
[6] Delbende I, Piton B and Rossi M 2015 *Eur. J. Mech. B Fluids* **49** 363
[7] Meunier P and Leweke T 2005 *J. Fluid Mech.* **533** 125
[8] Meunier P, Le Dizès S and Leweke T 2005 *C. R. Physique* **6** 431
[9] Leweke T, Le Dizès S and Williamson C H K 2016 *Annu. Rev. Fluid Mech.* **48** 507
[10] Meunier P and Leweke T 2001 *Phys. Fluids* **13** 2747
[11] Leweke T, Quaranta H U, Bolnot H, Blanco-Rodríguez F J and Le Dizès S 2014 *J. Phys. Conf. Ser.* **524** 012154
[12] Schröder D, Leweke T, Hörnschemeyer R and Stumpf E 2021 *AIAA SciTech Forum* Paper 2021-1088
[13] Rayleigh L 1917 *Proc. R. Soc. Lond.* A **93** 148
[14] Billant P and Gallaire F 2005 *J. Fluid Mech.* **542** 365
[15] Billant P and Gallaire F 2013 *J. Fluid Mech.* **734** 5
[16] Bayly B J 1988 *Phys. Fluids* **31** 56
[17] Ash R L and Khorrami M R 1995 *Fluid Vortices* ed Green S I (Dordrecht: Springer) p 317